Journal of Hazardous Materials 190 (2011) 729–737

Contents lists available at ScienceDirect

Journal of Hazardous Materials

journal homepage: www.elsevier.com/locate/jhazmat

Biodegradation of *p*-nitrophenol using *Arthrobacter chlorophenolicus A6* in a novel upflow packed bed reactor

Naresh Kumar Sahoo [a], Kannan Pakshirajan [b], Pranab Kumar Ghosh [c,*]

[a] *Center for the Environment, Indian Institute of Technology Guwahati, 781039, India*
[b] *Department of Biotechnology, Indian Institute of Technology Guwahati, 781039, India*
[c] *Department of Civil Engineering, Indian Institute of Technology Guwahati, 781039, India*

ARTICLE INFO

Article history:
Received 12 January 2011
Received in revised form 28 March 2011
Accepted 29 March 2011
Available online 4 April 2011

Keywords:
p-Nitrophenol
Arthrobacter chlorophenolicus A6
Packed bed bioreactor
Polyurethane foam
PUF
PNP

ABSTRACT

A novel packed bed reactor (PBR) was designed with cross flow aeration at multiple ports along the depth to improve the hydrodynamic conditions of the reactor, and the biodegradation efficiency of *Arthrobacter chlorophenolicus A6* on p-nitrophenol (PNP) removal in PBR at different PNP loading rates were evaluated. The novel PBR was designed to improve the hydrodynamic features such as mixing time profile (t_{m95}), oxygen mass transfer coefficient (k_La), and overall gas hold up capacity (ε_G) of the reactor. PNP concentration in the influent was varied between 600 and 1400 mg l^{-1} whereas the hydraulic retention time (HRT) in the reactor was varied between 18 and 7.5 h. Complete removal of PNP was achieved in the reactor up to a PNP loading rate of 2787 mg l^{-1} d^{-1}. More than 99.9% removal of PNP was achieved in the reactor for an influent concentration of 1400 mg l^{-1} and at 18 h HRT. In the present study, PNP was utilized as sole source of carbon and energy by *A. chlorophenolicus A6*. Furthermore, the bioreactor showed good compatibility in handling shock loading of PNP.

1. Introduction

The presence of substituted groups in phenol particularly nitro, chloro and bromo increases its toxic effects exerted on the environment as well as on the human health owing to their carcinogenic and recalcitrant properties [1]. The U.S. environmental protection agency (EPA) has listed *p*-nitrophenol (PNP) as a priority pollutant and recommended its concentrations in natural waters and drinking waters to below 10 ng l^{-1} [2,3] whereas, monthly average industrial effluent concentrations of PNP should not exceed 162 μg l^{-1} [4]. PNP is probably the most important among the mono-nitrophenols in terms of its annual usage which is up to 20 million kg per year [5]. The major sources of wastes that discharge PNP are the industries mainly involved in the management of explosives, drugs, dyes, phosphoorganic insecticides (methyl parathion), pesticides and leather. PNP are also formed in aqueous matrices during pesticides formulation, distribution and field application [6]. In addition, PNP was detected in rain water in Japan, which forms due to photochemical reaction between benzene and nitrogen monoxide in the atmosphere [7]. It may also have the potential to leach through soil and enter groundwater, where they are hardly degradable and hence persist in the environment [8]. All these aspects warrant a high efficiency treatment of wastewaters contaminated with PNP and other substituted phenols prior to their discharge into the environment. Although several techniques such as volatilization, photo-decomposition, physical adsorption, solvent extraction, chemical oxidation and electrochemical methods have been tested for the removal of phenol and phenolic compounds from wastewaters [9], high cost, low efficiency and generation of toxic by-products are some of the limiting factors of these methods. The eco-friendly biodegradation process has gained maximum attention due to its many advantages over the traditional physico-chemical methods. However, the presence of nitro groups enhances the resistance of the aromatic ring against biodegradation by many microorganisms [1,10,11], and hence only selective species of bacteria belonging to *Flavobacterium*, *Alcaligenes*, *Pseudomonas*, *Rhodococcus* and *Arthrobacter* have shown ability to degrade PNP [10–12]. Among these microbial species, actinomycetes secrete both extracellular as well as intracellular enzymes and have thus revealed good potential in degrading PNP more effectively. *Arthrobacter chlorophenolicus A6* is an aerobic actinomycetes that has been demonstrated to degrade wide different types of toxic substituted phenols in batch shake flask and is also reported to be one of the most efficient strains that completely mineralize 4-chlorophenol (4-CP) even at 300 mg l^{-1} within 24 h of culture [13]. However, there is also no report available so far on the performance of *Arthrobacter chlorophenolicus A6* on

* Corresponding author. Tel.: +91 361 2582418; fax: +91 361 2692440.
E-mail addresses: pkghosh@iitg.ernet.in, pranab_k_ghosh@rediffmail.com (P.K. Ghosh).

0304-3894/$ – see front matter © 2011 Elsevier B.V. All rights reserved.
doi:10.1016/j.jhazmat.2011.03.106

biodegradation of PNP in any kind of bioreactor. Moreover, all the studies conducted so far on PNP degradation using microorganism have been largely limited to experiments in simple batch shake flasks except only for a few on stirred tanks, and sequencing batch reactor [14–17]. Furthermore, the performances of these reactors were largely limited under high PNP loading conditions.

Biofilm reactors have certain advantages over suspended growth bioreactors as it offers higher resistance to shock loads and its ability to survive even at low influent substrate concentrations. Besides, biofilm reactors offer high volumetric biomass concentration in small reactor volume [18]. Packed bed reactor (PBR) is one such biofilm reactor that has gained much popularity in wastewater treatment. Furthermore, packed bed reactor (PBR) operating in upflow mode prevents the suspended biomass wash out as well as reduces frequent clogging in comparison to down flow PBR. However, when a PBR is operated in an upflow mode with the supply of oxygen from the bottom of the reactor, gas channeling occurs leading to the development of liquid-rich and gas-rich regions rather than uniform distribution of oxygen and food throughout the reactor bed [19,20]. Furthermore, reduction of pressure drop and superficial flow velocity diminish the growth of microorganisms and thereby degradation of organic pollutants due to lack of availability of sufficient oxygen and/or food deep inside the reactor bed material, especially when the bed contains a porous but poorly permeable supporting material for the growth of microorganisms [21,22]. Therefore, hydrodynamic conditions in a PBR need to be improved to get maximum microbial growth and degradation efficiency. One possible way to achieve this could be through introduction of cross flow system with aeration through multiple numbers of ports, (fragmented approach) along the length of a PBR. The present study investigated the performance of a novel packed bed bioreactor designed with cross flow aeration at multiple ports for PNP removal by *Arthrobacter chlorophenolicus A6* at different feeding and operational conditions.

2. Materials and methods

2.1. Materials

All the chemicals and reagents used were either of analytical reagent (AR) grade or laboratory reagent (LR) grade. AR grade *p*-nitrophenol (PNP) was procured from Himedia (India).

2.2. Analytical methods

Biomass concentration in samples was determined by measuring optical density at wavelength 600 nm (OD_{600}) using a UV–vis spectrophotometer (Model lambda-45, Perkin Elmer, USA). The absorbance values were expressed as dry cell weight using a calibration curve plotted between the optical density (OD_{600}) versus mixed liquor suspended solids (MLSS) of the sample. One unit of absorbance was found equivalent to 235 mg l^{-1} of MLSS. Biomass concentration on the support material, PUF, was measured by following Bradford method of protein assay [23]. About 1 g of PUF was dried at 105 °C for 12 h and soaked in a 1 M NaOH solution, which was then digested at 90 °C for 10 min. After cooling, the Bradford protein assay was performed. A calibration curve relating biomass dry weight to protein concentration was obtained. Chemical oxygen demand (COD) of samples was measured by closed refluxed methods following the procedure recommended in standard methods [24]. PNP concentration in biomass free samples was estimated using reverse phase HPLC (Varian Prostar 210) equipped with an Onsphere 5-pesticides C-18 column (Varian) using methanol-water and acetic acid (50:49.1, v/v) as the mobile phase. The retention time of PNP was found to be 3.1 min at a flow rate of 0.4 ml min^{-1}. PNP concentration was measured in the HPLC equipped with a UV–vis detector at wavelength 280 nm. For the identification of PNP biodegraded intermediates the samples were analyzed using LC/MS (WATERS LC-MS/MS system, Q-Tof Premier). A capillary ACQUITY UPLC® BEH shield RP 181.7 μm C-18 column (10 mm × 50 mm length) was used for separation of product intermediates. The mobile phase was a mixture of acetonitrile–water–formic acid (1:1:0.1, v/v) filtered through Millipore syringe filter of 0.22 μm.

2.3. Toxicity test

Resazurin reduction method was used [25] to determine the percentage toxicity removal at the optimum loading rate of 2787 mg l^{-1} d^{-1} of novel PBR. *A. chlorophenolicus A6* and mixed microbial consortia, collected from a municipal wastewater treatment plant were used as test organisms. Following equations were used to calculate % toxicity and % toxicity removal:

$$\%\ \text{toxicity} = \left(\frac{A-B}{C-B}\right)$$

where A = optical density (OD) of the test tubes containing influent or effluent wastewater; B = OD for the cell tube (cells + water with no PNP); and C = OD for the control tube (only water).

Percent toxicity removals were calculated as:

$$E = 1 - \left[\frac{\%\ \text{Toxicity}_e}{\%\ \text{Toxicity}_i}\right]$$

where "% Toxicity_e" and "% Toxicity_i" are the percentage toxicities of the effluent and the influent, respectively, with respect to control.

2.4. Microscopic methods

Fragments of polyurethane foam (PUF) containing the microbial biofilm were sampled at various points of the packed bed and cut into small thin pieces. Scanning electron micrograph (SEM) images of samples glued on an aluminium stub and gold sputtered were obtained by means of a LEO-1430 VP (Japan) electron microscope.

2.5. Experimental setup of the packed bed bioreactor

A laboratory scale packed bed bioreactor was fabricated using a perspex cylinder of height 60 cm and internal diameter 11.6 cm as the main reactor unit and PUF as supporting material for microbial growth. Working volume in the reactor was 4 l. Detailed specification of the reactor and its various components are presented in Table 1. Porosity of PUF was determined according to the method

Table 1
Detailed specifications of the reactor.

Total reactor volume	6 l
Liquid working volume	4 l
Height of aeration port	At each 10 cm
Circular porous perplex disc	5 mm pore size
Nylon membrane	0.25 mm pore size
Fixed bed height	40 cm
Intra-particle porosity, ε_p	0.716
Inter-particle porosity, ε_e	0.2096
Total bed porosity, $\varepsilon_{tot} = \varepsilon_e + \varepsilon_p$	0.9255
Dry material bulk density, ρ_{tz} (g cm^{-3})	0.033
Packed-bed volume, V_{PB} (cm^3)	4000
Packed-bed void volume, $V_{void} = V_{PB}(\varepsilon_e + \varepsilon_p)$ (cm^3)	3702
Packed-bed circulating liquid volume, $V_{PB}(\varepsilon_e)$ (cm^3)	838
Packed-bed stagnant liquid volume, $V_{PB}(\varepsilon_p)$ (cm^3)	2864

ε_e = inter particle porosity; ε_p = intra particle porosity; $\varepsilon_{tot} = \varepsilon_e + \varepsilon_p$ total bed porosity; ε_G = gas hold-up (%); $V_{PB} = V_D$ packed-bed volume (l); t_{m95} = time to reach 95% homogeneity after a tracer input(s); U_{GR} = superficial air velocity in riser (cm s^{-1}); $V_{void} = V_{PB}(\varepsilon_e + \varepsilon_p)$ void volume of packed-bed (l); k_{La} = mass transfer coefficient in (h^{-1}).

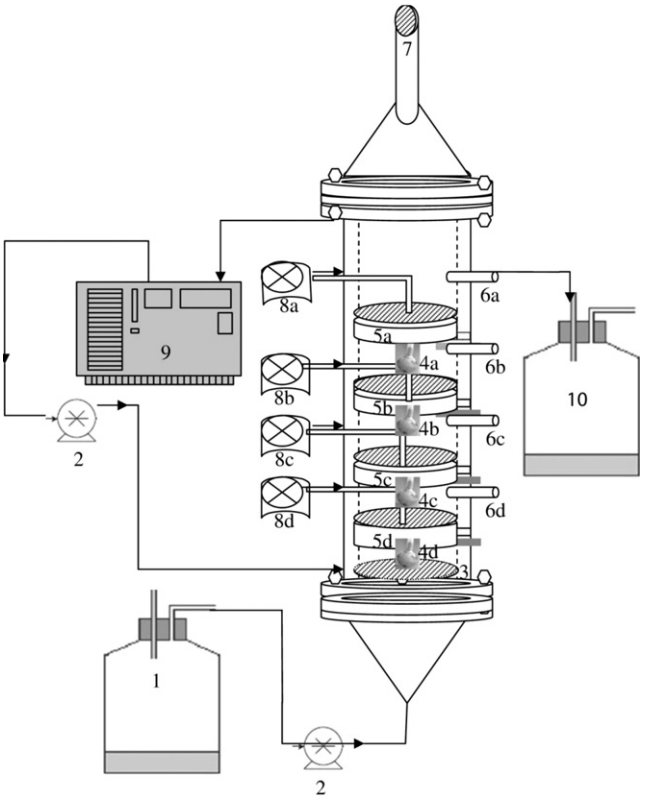

Fig. 1. Schematic of the experimental set up of the novel PBR with its various components: (1) Influent tank, (2) peristaltic pump, (3) wire gauze, (4) a, b, c and d, ceramic gas diffuser, (5) a, b, c and d, perforated perspex disc with its top wrapped with nylon mesh, (6) a, b, c and d sampling port, (7) gas outlet, (8) a, b, c and d aeration pumps, (9) water bath, and (10) effluent reservoir.

described by Hodge and Devinny [26]. For sampling as well as for aeration, different ports were provided at every 10 cm along the height of the reactor. Inert PUF was cut into approximately (2.5 cm × 1.5 cm × 1.5 cm) cubes, washed twice with double deionized water, autoclaved (20 min, 120 °C), rewashed, and dried overnight at 70 °C in a hot air oven before being used as bio-support material in the packed bed reactor (PBR). 100 g of oven dried PUF of was placed inside the reactor. Aeration from an air compressor was provided in the reactor through ceramic diffusers at varying air flow rates from 2 to 10 l min^{-1}. The aeration rate was monitored using a digital flow meter (Flow-tech engineers, Mumbai, India). The reactor was fed with synthetic wastewater containing PNP at controlled flow rate using a peristaltic pump (Model: pp10, Miclins India). The temperature inside the reactor was maintained at 29 ± 1 °C by circulating warm water from a thermostat installed temperature controlled water bath (JCSW Mumbai, India) through plastic pipes wrapped over the reactor throughout its length. A schematic of the bioreactor is depicted in Fig. 1.

2.6. Hydrodynamic experiments with the PBR

Hydrodynamic experiments were performed with the PBR under two different aeration systems viz., aeration only through the bottom aeration port and aeration through all the 4 ports to achieve cross flow aeration. The reactor operated under the first condition (aeration through single port) was designated as "simple PBR", whereas, the reactor operated under the second condition (aeration through all the 4 ports) was designated as "novel PBR". In the first case, no perforated circular disks were used in the reactor whereas, in the latter case 4 nos. of perforated circular discs wrapped with nylon mesh at the top were placed just above the ceramic porous stones through which oxygen (air) was diffused into the reactor content by supplying compressed air from an air compressor.

2.6.1. Mixing time profile

Mixing time in both the conditions of the reactor was determined using a tracer technique that measured pH change in a pre-homogenized solution after an acid pulse [27]. The simple PBR was first filled up with 0.15 N NaCl solution before an aliquot of 6 N HCl (2.0 ml) was injected at the bottom of the reactor at four different superficial gas flow rates of (cm s^{-1}); 0.078, 0.157, 0.236, 0.315. The effluent pH was then measured at different time intervals using a pH meter (Sartorius, USA). The experiment was repeated for novel PBR after the acid retained by the support material in the reactor was washed out by draining and rinsing the bed three times with distilled water. The transitory changes in the relative values of pH (ΔpH[t]), were estimated using the following relation:

$$\Delta \mathrm{pH}[t] = \frac{\mathrm{pH}[t] - \mathrm{pH}_0}{\mathrm{pH}_0 - \mathrm{pH}_\infty} \quad (1)$$

where pH[t] represents pH at time [t], pH_0 is initial pH and pH_∞ represent pH at infinitive time or saturated pH value.

By plotting ΔpH[t] data, t_{m95} (i.e. time to reach 95% homogeneity after a tracer input (s)) was estimated for each value of U_{GR} (superficial air velocity, cm s^{-1}) in the reactor.

2.6.2. Oxygen mass transfer coefficient determination

The oxygen mass transfer coefficients in both the operating conditions of the reactor (i.e. simple PBR and novel PBR) were determined by classical dynamic gassing-in method under abiotic condition (i.e. before inoculation of microorganism) [28]. In this method, the PBR was filled up with 0.15 N NaCl solution and then the dissolved oxygen was removed by purging nitrogen gas. The initial DO was measured (Model: HQ 40d HACH, USA) and oxygen was supplied in the form of air through the bottom aeration port only (simple PBR condition), to raise the DO level in the reactor. Effluent DO concentration was measured at different time intervals until DO level saturated in the reactor. The experiment was performed at two different superficial air flow rates of 0.157 and 0.315 cm s^{-1}. The experiment was repeated by supplying air through all the four aeration ports to determine the oxygen mass transfer coefficient in the novel PBR. Oxygen supply rates into the reactor in the above two conditions (simple and novel PBR) were, however, maintained the same. The oxygen balance in the reactor was expressed in its integrated form as given below by assuming negligible resistance due to the DO sensor:

$$\ln(C_S - C_L) = -k_L a t + \ln(C_S - C_{L0}) \quad (2)$$

where C_S is the saturated DO concentration, C_L and C_{L0} are the bulk DO concentration at any time t and $t = 0$, respectively. The values of $k_L a$ in each experiment were obtained from the slope of $\ln(C_S - C_L)$ vs t.

2.6.3. Gas holdup determination

The overall gas holdup (ε_G) in both the conditioned of reactor run (i.e. simple PBR and novel PBR) was measured by volume expansion method [29] using the following expression:

$$\varepsilon_G = \frac{\Delta V}{\Delta V + V_{LS}} \quad (3)$$

where V_{LS} represents the liquid volume in both the packed bed system; ΔV was the volume expansion after gas dispersion, calculated by multiplying the average change in liquid level (height) in the reactor with the cross-section area of the reactor.

2.7. Abiotic PNP removal in the novel packed bed bioreactor

Experiment was carried out to estimate the abiotic loss of PNP in the reactor due to adsorption onto bio-support material, and volatilization with air supplied into the reactor. As mentioned earlier, PUF was used as supporting material in the pack bed reactor (PBR). There are several reports on removal of various pollutants through adsorption on PUF [30]. In order to estimate abiotic PNP removal, the novel bioreactor was operated without aeration by supplying wastewater containing 200 mg l^{-1} of PNP in optimized mineral salt medium (MSM) having the composition (g l^{-1}): K_2HPO_4 2.6; KH_2PO_4 0.4; NH_4NO_3 0.58; $MgSO_4$ 0.17; $CaCl_2$ 0.038 and $FeCl_3$ 0.002 [31]. The HRT of the reactor was maintained at an arbitrary value of 10 h. When both effluent and influent PNP concentrations were the same, the reactor was aerated through all the four ports to estimate PNP loss due to volatilization. All the experiments were carried out at temperature 29 ± 1 °C.

2.8. Seed culture medium and biofilm development

A chlorophenolicus A6 used in the present study for PNP biodegradation was a kind gift from Prof. Janet K. Jonson, Department of Biochemistry, Stockholm University, Sweden. The media used for developing the seed culture contained MSM reported by Alexandar and Lustigman [32]. The MSM was added with 0.1% of yeast extract and 150 mg l^{-1} of 4-chlorophenol (4-CP). The seed culture medium of 100 ml was taken in a 250 ml Erlenmeyer flask, and was inoculated with a loop full of the culture freshly grown on agar slants and incubated in an incubator shaker for 48 h at 30 °C and 180 rpm. The seed culture cells were centrifuged (5000 × *g*, 20 min at 22 °C), washed in sterile phosphate buffer (pH 7.4), and regrown overnight in optimized minimal salts medium as described by Sahoo et al. [31] with 200 mg l^{-1} of PNP as the sole source of carbon and energy. The active cells were again centrifuged (5000 × *g*, 20 min at 22 °C), washed with 1× phosphate buffer saline (pH 7.4), and suspended in four liter of optimized MSM [31] with 200 mg l^{-1} of PNP to give a cell suspension of 0.75 OD_{600}. The cell suspension was inoculated by pumping into the reactor packed with PUF cubes by means of a peristaltic pump (Model: pp10, Miclins India). Any biomass washed out of the reactor along with the effluent was recycled back. The reactor was continuously fed with the above mentioned MSM spiked with varying PNP concentrations varying between 200 and 600 mg l^{-1} and was operated for about 1 month at different flow rates to maintain different HRT of 18–12.5 h, until sufficient biomass concentration and steady state performance was achieved. To confirm the biomass in the PBR, a few cubes of PUF (biosupport material) was sampled for microscopic analysis as mentioned earlier.

2.9. Optimization of dissolved oxygen level in the reactor

Dissolved oxygen concentration can affect the synthesis of enzymes for which oxygen is a substrate, growth rates, and on the regulation of gene expression [33]. In the present study, performance of the reactor operated at different DO level was monitored for its optimization, and the experiment was performed after allowing sufficient biomass growth in the reactor which took almost 1 month. The reactor was operated at 12.5 h of HRT with an influent PNP concentration of 600 mg l^{-1} that was equal to a PNP loading rate of 1264 mg l^{-1} day^{-1}. Aeration rate was varied between 2 and 10 L min^{-1} to achieve different DO levels in the range 2–7 mg l^{-1}. At each DO level the experiment was carried out until a steady state condition was achieved that took about 2 days.

2.10. PNP biodegradation experiments with the novel PBR

The performance of the novel PBR on PNP biodegradation was studied at optimum DO level by controlled supply of air. The temperature of the reactor was maintained at an optimum value of 29 ± 1 °C [34]. The synthetic wastewater (pH 7.5) contained optimized MSM [31] with varying concentrations of PNP (600–1400 mg l^{-1}) as the sole source of carbon and energy. The wastewater was fed into the reactor at varying flow rates with the help of a peristaltic pump to maintain different HRT between 18 and 7.5 h. The operational schedule of the reactor is given in Table 2. Shock loading experiments were also performed at two different conditions of sudden increase in PNP loading rate from 842 and 2247 mg l^{-1} d^{-1} to 1966 and 4492 mg l^{-1} d^{-1}, respectively. Samples were taken at regular time interval and analyzed for biomass, COD and PNP concentrations.

3. Results and discussions

3.1. Hydrodynamic study in novel PBR

As described earlier, the hydrodynamic experiment was performed in PBR under two different aeration systems viz., aeration only through the bottom aeration port (simple PBR); and aeration through all the 4 ports with the arrangement to get cross flow aeration along with perforated discs wrapped by nylon membrane at the top (novel PBR). Fig. 2 compares the results of hydrodynamic study performed in these two conditions of the reactor. Fig. 2(a) shows the mixing profile in the novel PBR which clearly reveals a better t_{m95} value (time to reach 95% homogeneity after a tracer input) of 110 s compared with 185 s in the simple PBR. This could be attributed due to its reduction of bubble formation, gas channeling effect and improved uniform dispersion of liquid and gas throughout the bed of the novel PBR. The mixing time (t_{m95}) obtained in both the reactors were plotted against the corresponding superficial gas flow velocity and are depicted in Fig. 2(b). The novel PBR had lower mixing time (t_{m95}) than the simple PBR for all the four gas flow rates investigated. This indicates a better liquid circulation rate in the novel PBR than the simple PBR. The maximum difference in t_{m95} was observed when the superficial gas flow velocity was 0.315 cm s^{-1}. At this condition the mixing time (t_{m95}) in the novel PBR and simple PBR were 99 and 175 s, respectively. Fig. 2(c) compares the values of oxygen mass transfer coefficient between the novel PBR and simple PBR. There was an enhancement of around 40% in k_La values in the novel PBR; from 97 to 139 h^{-1}, and 54 to 76 h^{-1} at the two different superficial gas flow rates of 0.315 and 0.157 cm s^{-1}, respectively. This could be attributed to the reduction in pressure drop leading to enhancement in gas flow velocity in the novel PBR. It is reported that cross flow design by multiple points along the height in packed beds reduces pressure drop enabling the use of practical flow rates and even flow distribution across wide packed bed [35]. In addition, due to the separation of the aeration zone (fragmented approach) at four levels along the height in the novel PBR presented a low shear stress compared to simple PBR at higher aeration rate using a single port [36] as a result reduced erosion of the immobilized biomass on the PUF and enhanced biomass density for better biodegradation efficiency. Fig. 2(d) shows the overall gas hold up profile in both the reactors at 4 different superficial gas flow velocities, which reveals a higher value of gas hold up in the novel PBR than the simple PBR. A maximum of 17% enhancement in overall gas hold up (from 6.9 to 8.35) was observed in the novel PBR for a superficial gas flow velocity of 0.315 cm s^{-1}. The increase in overall gas hold up capacity (ε_G) in the novel PBR may be due to the reduction in pressure

Table 2
Operational schedule of the PBR.

PBR operation period (day)	HRT (h)	Influent conc. (mgl^{-1})	PBR operation period (day)	HRT (h)	Influent conc. (mgl^{-1})
0-13*[a]	12.5	600	63-66	7.5	1200
13-16*[b]	18	600	66-71	18	1400
16-19	12.5	600	71-75	12.5	1400
19-21	10	600	75-78	10	1400
21-24	7.5	600	78-80	7.5	1400
24-28	18	800	80-88*[c]	18	600
28-31	12.5	800	88-90	18	600
31-34	10	800	90-92	18	1400
34-37	7.5	800	92-94	18	1400
37-41	18	1000	94-96	18	1400
41-44	12.5	1000	96-102	7.5	600
44-47	10	1000	102-104	7.5	1200
47-51	7.5	1000	104-106	7.5	1200
51-55	18	1200	106-108	7.5	1200
55-59	12.5	1200	108-111	7.5	1200
59-63	10	1200	111-114	7.5	1200

*abc: PBR operational schedule during DO optimization, reactor performance evaluation and shock loading conditions

drop as a result of more volume expansion (ΔV) and greater gas hold up. An increase in overall gas holdup could also have affected the gas–liquid interfacial area and thus the oxygen mass transfer coefficient.

3.2. Abiotic PNP removal by adsorption and volatilization

PNP removal in PBR by adsorption onto PUF was estimated from the breakthrough curve shown in Fig. 3. As shown in the figure, the

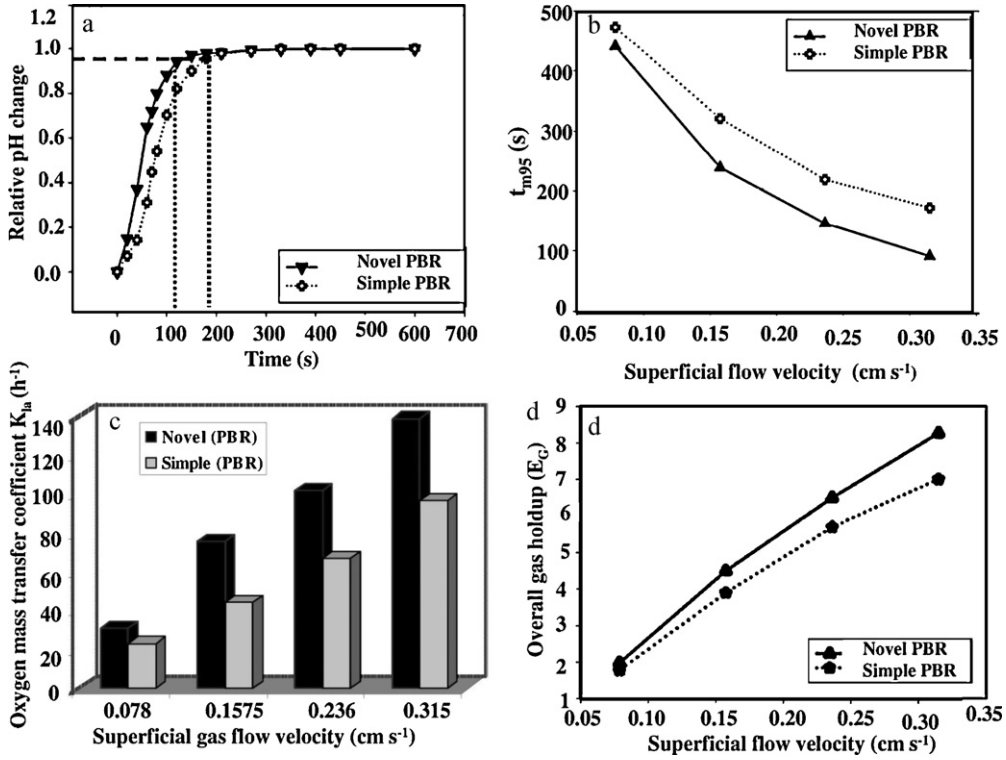

Fig. 2. Comparison of hydrodynamic profiles obtained using the novel and simple PBRs in the study: (a) mixing time profile at superficial flow velocities (U_{GR}) = 0.315 cm s^{-1}; (b) mixing time behavior at varying superficial air flow velocities; (c) oxygen mass transfer coefficients (k_La) at U_{GR} values of 0.1575 and 0.315 cm s^{-1}; (d) overall gas hold-up at different air flow velocities.

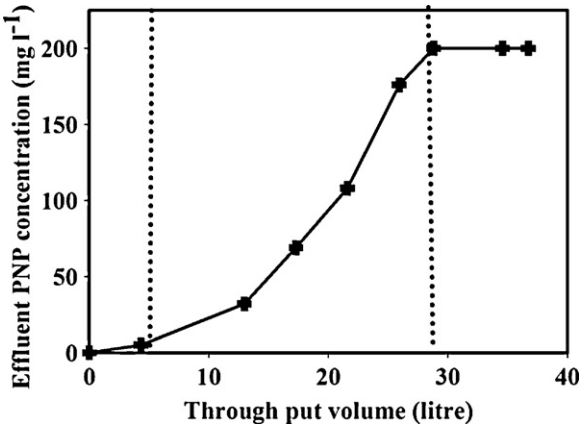

Fig. 3. Breakthrough curve obtained for determining the adsorption capacity of the biosupport material used in the novel PBR (PNP influent concentration = 200 mg l^{-1}, HRT = 10 h).

bed was saturated at the end of 80 h of operation showing effluent PNP concentration was almost equal to the influent PNP concentration. Thus, the adsorption capacity of PNP was calculated to be 37.84 mg of PNP g^{-1} dry weight of PUF, which was much less than the adsorption capacity of activated carbon. With an initial PNP of 278 mg l^{-1}, adsorption capacity of activated carbon for PNP was calculated to be 556.44 mg of PNP g^{-1} activated carbon [37]. PNP removal due to volatilization was about 3 mg l^{-1} (1.5%) at an influent PNP concentration of 200 mg l^{-1} and aeration rate of 8 L min^{-1}, Several researchers reported insignificant to very less loss of PNP via volatilization [38,39].

3.3. SEM characterization of PUF

Fig. 4 shows the scanning electron microscopic (SEM) images of PUF before and following the growth of *Arthrobacter chlorophenolicus A6*, which confirms microbial colonization on the biosupport material. Observation of the biosupport matterial using SEM showed a succession of densely colonized areas shown in Fig. 4(b). Closer examination of the surface revealed the presence of dense biofilms embedded within a polymeric matrix (Fig. 4(c)) and most colonies were observed to be large sized and cocci shaped.

3.4. Optimization of DO concentration

Fig. 5 presents the effect of DO on PNP removal in the novel PBR at the PNP loading rate of 1264 mg l^{-1} day^{-1}. The PNP removal efficiency was found to be the maximum when DO in the reactor was within the range of 4.9 and 5.5 mg l^{-1} which is in close agreement with the literature reports [40]. However, any further increase in the DO concentration did not improve the PNP removal efficiency in the novel PBR system. This might be due to the fact that at higher DO level, the oxygen acts as a strong electron withdrawing group inherent to nitro-aromatics and reduces the electron density of the aromatic ring resulting in inhibition of oxidative attack by the electrophilic oxygenases [41]. The reduction in the reactor performance at lower DO level may also be due to the inadequate transfer of DO to the microorganisms present deep inside the biofilm formed in the pores of the PUF, causing anaerobic conditions [42]. The first 13 days of operation shown in Fig. 6 represents the experiment related to optimization of DO concentration.

3.5. PNP biodegradation in the novel PBR

The operational schedule of the PBR is given in Table 2 and the performance of the reactor on PNP biodegradation is shown in Fig. 6.

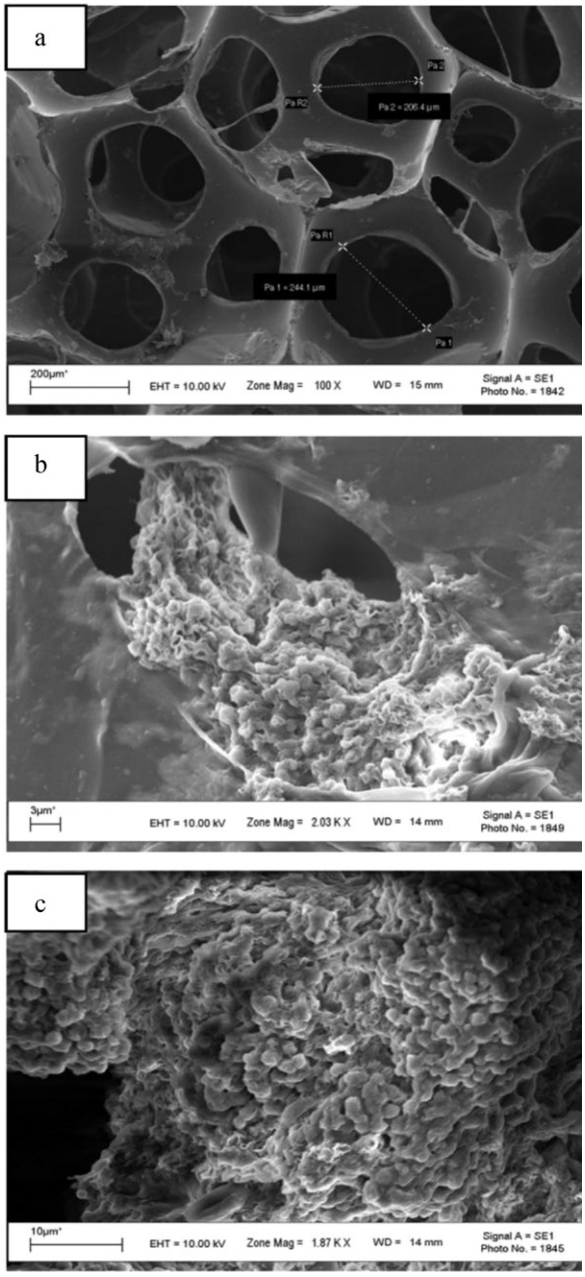

Fig. 4. SEM images of PUF: (a) vesicular structure of PUF before inoculums, (b) bacterial growth on PUF, and (c) magnified picture of (b) showing more clear bacterial morphology.

The reactor was started with 600 mg l^{-1} of PNP in the influent and was operated with stepwise increase in PNP concentrations up to 1400 mg l^{-1} for a total period of 114 days at varying HRTs of 18, 12.5, 10, and 7.5 h. Change in HRT and/or influent PNP concentration was done once the reactor acquired steady state condition. PNP was the sole carbon source added into the reactor which has a chemical oxygen demand (COD) of 1.69 mg l^{-1}. The reactor was able to reduce PNP to below detection limit even at the shortest HRT of 7.5 h. The organic carbon removal in the reactor measured as COD was even more than 98% when operated at an influent PNP of 1000 mg l^{-1} suggested that the PNP was utilized by the microorganisms as sole source of carbon and energy. At the influent concentrations of 800 and 1000 mg l^{-1}, complete PNP removal was noticed when HRT was 10 h or more. However, the reactor could not completely remove PNP when the HRT was lowered to 7.5 h. The effluent PNP

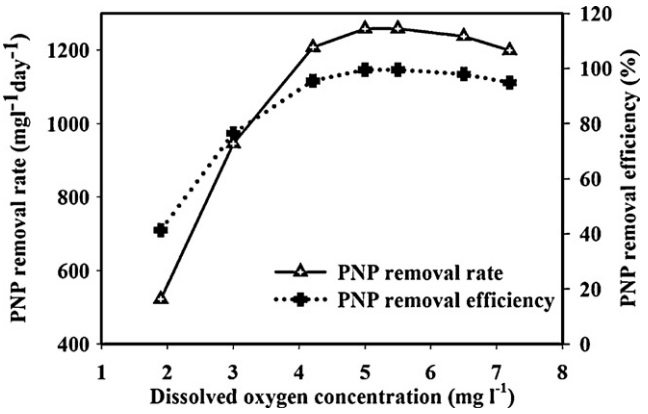

Fig. 5. Dissolved oxygen profile with respect to PNP removal rate and removal efficiency at a constant loading rate of 1264 mg l^{-1} day^{-1}.

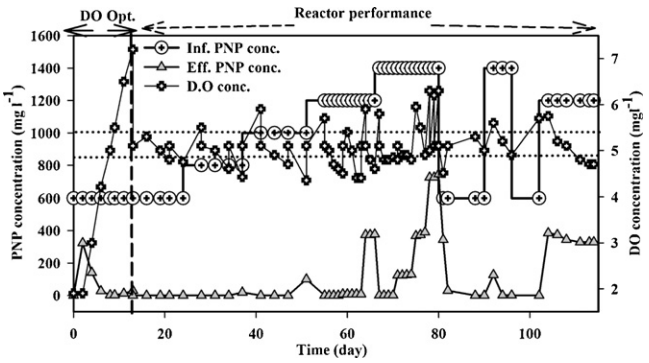

Fig. 6. PNP biodegradation profile in the novel PBR.

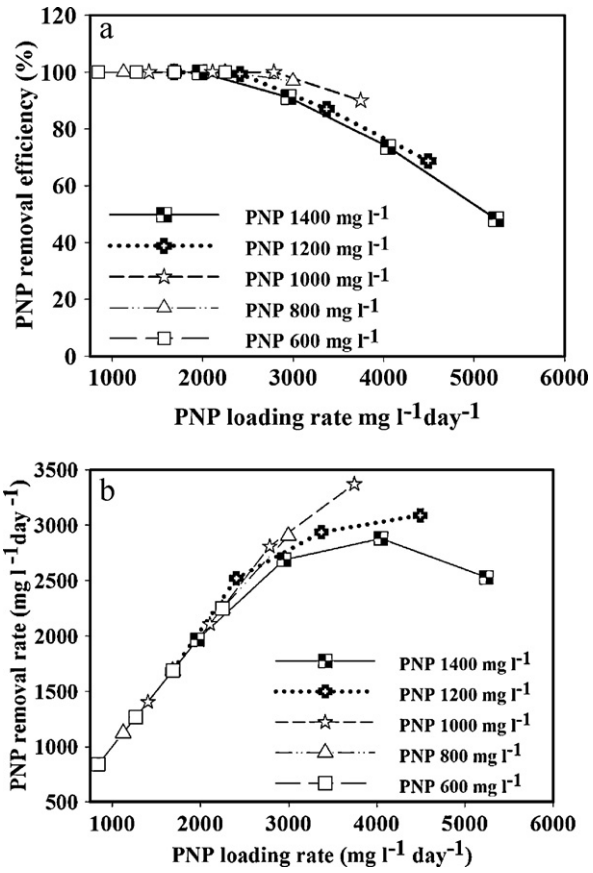

Fig. 7. (a) PNP removal efficiency, and (b) PNP biodegradation rate in the novel PBR at different PNP loading rates.

concentrations were about 20 and 100 mg l^{-1}, respectively. Furthermore, at the influent concentrations of 1200 and 1400 mg l^{-1}, the reactor could remove more than 99.5% of PNP when operated at the HRTs of 12.5 and 18 h, respectively. The reactor performance was drastically reduced at HRTs lower than 10 h and influent PNP concentrations greater than 800 mg l^{-1}.

DO profile during the operational period of the reactor is also shown in Fig. 6. Two dotted lines parallel to *X* axis represents the optimum DO concentration range between 4.9 and 5.5 mg l^{-1}. Whenever DO in the reactor content was beyond this range it was brought back to this range by controlling rate of supply of air into the reactor. Sudden decrease or increase in DO concentration in the reactor was noticed due to change in organic loading rate either by changing HRT, or PNP concentration in the feed, or by changing the both. Sudden decrease in DO concentration in the reactor were noticed whenever there was an increase in PNP loading rate due to lowering of HRT of the reactor fed with 600–1200 mg l^{-1} of PNP. This might be due to sudden increase in DO demand by the microorganism to degrade the extra amount of PNP introduced to maintain a lower HRT. Similarly, sudden increases in DO concentration were noticed on 24th, 37th, 51st and 66th days as PNP loading rate was decreased due to increase in HRT from 7.5 to 18 h, even if the PNP concentration in wastewater was enhanced stepwise from 600 to 800, 1000, 1200 and 1400 mg l^{-1}, respectively (Table 2). Similar change in DO profile has been observed by other researchers [43]. Although, the DO level could be brought back to a value near 5 mg l^{-1} by controlling air supply, a prominent ascends in DO concentration was observed on 75th day of run (Fig. 6) when the reactor was introduced with wastewater containing 1400 mg l^{-1} of PNP and an HRT of 10 h (Table 2). This might be due to the toxicity effects of PNP at this concentration that inhibited the microorganisms from normal metabolic activities leaving significant amount of DO and PNP unutilized. Percentage PNP removal was only 74% at this condition. Performance of the reactor was even worse when the HRT was lowered to 7.5 h, where PNP removal was only 48%.

In fact, the reactor performance was greatly dependent on the PNP loading rate that depends upon PNP concentration and HRT. Experimental data are re-plotted in Fig. 7(a) and (b) to show the reactor performance in terms of percentage removal, and PNP removal rate (mg l^{-1} d^{-1}) respectively at different PNP loading rates. Fig. 7(a) shows that almost complete removal of PNP in the reactor was achieved at the maximum PNP loading rate of 2787 mg l^{-1} d^{-1} when the reactor was operated at 10 h HRT and 1000 mg l^{-1} influent PNP concentration. To the best of our knowledge, this is the maximum PNP loading rate at which complete removal of PNP was achieved in any bioreactor reported so far. In addition, the novel PBR removed PNP more than 99.9% from an initial concentration of as high as 1400 mg l^{-1} (HRT = 18 h). The maximum PNP concentration that was completely removed from any bioreactor so far is only 320 mg l^{-1} [6], whereas in any batch shake flask it is 500 mg l^{-1} [44]. Furthermore, the maximum PNP concentration investigated in any bioreactor so far with 99% degradation efficiency is 528.73 mg l^{-1} [15]; beyond this concentration the authors observed inhibition of the microorganism performance. However, at loading rates greater than 2787 mg l^{-1} d^{-1} PNP removal efficiency gradually reduced in the present study irrespective of the influent concentration. Though, complete PNP removal was observed at the PNP loading rate of 2787 mg l^{-1} d^{-1}, maximum PNP removal rate of 3371 mg lmg l^{-1} d^{-1} was obtained at the loading rate of 3746 mg l^{-1} d^{-1} (PNP = 1000 mg l^{-1}, HRT = 7.5 h) [Fig. 7(b)]. Fig. 7(b) also indicates that it could be possible to achieve better PNP removal rate had the reactor been operated at HRTs

lower than 7.5 h with an influent PNP concentration of 1200 mg l^{-1} or lesser. However, the reactor performance (% removal) decreased with increase in PNP loading rate leaving high PNP concentration in the treated effluent [Fig. 7(a)]. Thus, the optimum conditions of PBR operation was observed at the PNP loading rate of 2787 mg l^{-1} d^{-1} for an inlet concentration of 1000 mg l^{-1}. COD removal efficiency at this operating condition was more than 98%. *p*-Nitrocatechol and hydroxy-quinol, which are the common intermediate products of PNP biodegradation by *Bacillus sphaericus JS905* [11] and *Arthrobacter* species [45] were identified in the reactor effluents. However, the concentration of these intermediates can be expected to be low at this operating condition, as removal of COD from the reactor was more than 98%. Furthermore, at this optimum loading rate of PNP the toxicity removal efficiency tested on mixed microbial consortia, and *A. chlorophenolius A6* were found very high of 93% and 97%, respectively. The PNP removal rate value achieved in the present study using the novel PBR is superior to other bioreactors reported so far in the literature [15,16]. Rezouga et al. [15] reported 99% removal of PNP in an aerobic stirred tank bioreactor from an influent PNP concentration of 528.73 mg l^{-1}, which is equivalent to 1490 mg l^{-1} d^{-1} of PNP loading rate. An influent PNP concentration more than 528.73 mg l^{-1} reduced the reactor performance significantly. Though, sponge-like structure of PUF has poor gas permeability [46], the higher PNP degradation efficiency observed in this study might be due to the enhancement of hydrodynamic conditions and gas liquid flow velocity. Higher gas liquid flow velocity might have facilitated better penetration of food (substrate) and oxygen (electron acceptor) deep inside the biosupport (PUF) leading to higher biomass growth as high as 380.5 mg g^{-1} of PUF and thus better PNP biodegradation performance. Similar biomass growth immobilized in PUF for nitrobenzene biodegradation was reported by Fava et al. [30], however, they achieved comparatively less biomass growth of 136.19 mg dry biomass per gm of PUF. The higher biomass growth leads to enhance the rate and efficiency of PNP biodegradation is also well correlated with our earlier work that 4-chlorophenol biodegradation by the *A. chlorophenoloicus A6* is a growth associated process [31]. Furthermore, in the present study the adsorption capacity of PNP was calculated to be 37.84 mg of PNP g^{-1} dry weight of PUF, which is comparatively insignificant with literature report of 556.44 mg of PNP g^{-1} activated carbon at a influent PNP concentration of 278 mg l^{-1} [37]. In addition, at an aeration rate of 8 L min^{-1}, loss of PNP due to volatilization was only 3 mg l^{-1} for an influent PNP concentration of 200 mg l^{-1}. Therefore, it is evident that abiotic PNP removal was, much lower than the total removal observed due to presence of the microorganism. Hence, removal of PNP in the novel PBR can be well said to be due to biodegradation by *A. chlorophenolicus A6*. Furthermore, similar pattern of COD removal profile (not shown) to that of PNP removal suggests that the microorganism used PNP as sole source of carbon and energy.

Any industrial wastewater treatment plant undergoes different intermittent organic and pollutant loading conditions, when concentrations of its pollutants changes abruptly. Karim and Gupta [47] reported reduction in efficiency of PNP degradation from 96% to 89.7% when HRT was reduced from 30 to 12 h (and thus increased the loading rate) in an up flow anaerobic sludge blanket reactor. Performance of the novel PBR under shock loading conditions was evaluated by monitoring the reactor performance on PNB removal at two different shock loading conditions (Table 2). PNB concentration in the influent was reduced from 1400 to 600 mg l^{-1} and HRT was increased from 7.5 to 18 h after 91st days of reactor run (Table 2). The reactor was operated at this condition for 6 days where complete removal of PNP was observed, and following which the influent PNP was suddenly raised to 1400 mg l^{-1} with an increase in PNP loading rate from 842 to 1966 mg l^{-1} d^{-1}. Though the reactor was upset temporarily as the removal efficiency was

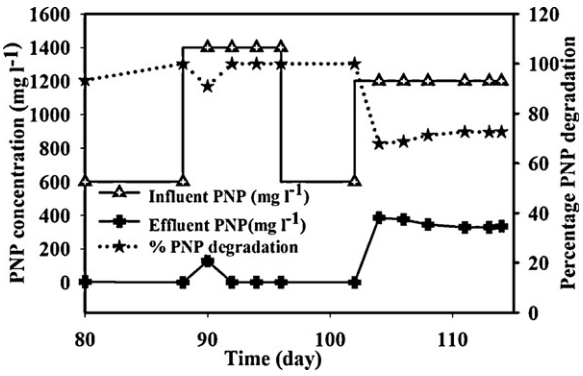

Fig. 8. PNP removal profile of the novel PBR under shock loading conditions.

only 91%, more than 99.9% PNP removal was observed only within 2 days of run, as shown in Fig. 8. The reactor was operated continuously at this condition for 2 more days and the performance was found to be stable. The operating conditions of the novel PBR was once again changed by reducing the influent PNP to 600 mg l^{-1} and HRT to 7.5 h on 105th day of the operation (Table 2). Complete removal of PNP was re-established within 2 days of operating of the reactor. The PNP in the influent was once again increased to 1200 mg l^{-1} but without any change in the HRT. Although the reactor performance was slightly disturbed due to this sudden change in operating condition, PNP concentration from 600 to 1200 mg l^{-1}, i.e. increases in PNP loading rate from 2247 to 4492 mg l^{-1} d^{-1}. However, the reactor performance was continued to improve till next 5 days and became stable with a removal efficiency of 74%. These results suggest that the novel PBR was able to completely regain its original performance within a short period of operation, under the two shock loading conditions tried, which is better performance compared with other continuous bioreactor systems tested for PNP biodegradation [16,48,49].

4. Conclusion

The novel PBR showed better hydrodynamic feature than the simple PBR. The polyurethane foams (PUF) with macro pores of sizes as large as 244 μm introduced in the reactor as support material for the growth of *Arthrobacter chlorophenolicus A6* had PNP adsorption capacity of 37.84 mg g^{-1}, which could remove PNP for only initial period of reactor operation. Complete removal of PNP was observed using the novel PBR at a maximum PNP loading rate of 2787 mg l^{-1} d^{-1}, which corresponded to PNP influent concentration of 1000 mg l^{-1} and 7.5 h HRT. *p*-Nitrocatechol and hydroxy-quinol were the main intermediates identified during PNP biodegradation process. About 98% COD removal under above operating condition suggested that accumulation of intermediates did not occur. Though, the reactor could remove more than 99% from 1400 mg/l influent PNP when operated at an HRT of 18 h, inhibition on *Arthrobacter chlorophenolicus A6* due to PNP was noticed at this influent concentration when operated at an HRT 10 h or less. Toxicity of PNP reduced the degradation of PNP and utilization of DO.

The present study demonstrated that the novel PBR is capable of not only 100% reduction of PNP in absence of any external carbon source but also highly efficient at a very high PNP loading rate of 2787 mg l^{-1} d^{-1}. In addition, the bioreactor showed good compatibility in handling shock loading of PNP in the system. Overall, the result obtained using the novel PBR displayed very high performance on treatment of PNP containing synthetic wastewater.

References

[1] V. Uberoi, S.K. Bhattacharya, Toxicity and degradability of nitrophenols in anaerobic systems, Water Environ. Res. 69 (1997) 146–154.
[2] M.R. Haghighi-Podeh, S.K. Bhattacharya, Q. Mingbo, Effects of nitrophenols on acetate utilizing methanogenic systems, Water Res. 29 (1995) 391–399.
[3] USEPA, Water Quality Criteria, Washington, DC, 1976.
[4] USEPA, Effluent Guidelines and Standards, Organic Chemicals, Plastics, and Synthetic Fibers, EPA/40 CFR Part 414, Washington, DC, 1988.
[5] B.A. Dolon, E. Razo-Flares, G. Lettiga, J.A. Field, Continous detoxification, transformation and degradation of nitrophenol in upflow anerobic sludge blacket (UASB) reactors, Biotechnol. Bioeng. 51 (1996) 439–449.
[6] M.C. Tomei, M.C. Annesini, R. Lubertia, G. Cento, A. Senia, Kinetics of 4-nitrophenol biodegradation in a sequencing batch reactor, Water Res. 37 (2003) 3803–3814.
[7] USEPA, Ambient Water Quality for Nitrophenols, EPA/440/5 80-063, Washington, DC, 1980.
[8] M. Trapido, J. Kallas, Advanced oxidation processes for the degradation and the detoxification of 4-nitrophenol, Environ. Technol. 21 (2000) 799–808.
[9] J.S. Ra, S.Y. Oh, B.C. Lee, S.D. Kim, The effect of suspended particles coated by humic acid on the toxicity of pharmaceuticals, estrogens and phenolic compounds, Environ. Int. 34 (2008) 184–192.
[10] F.K. Higson, Microbial degradation of nitroaromatic compounds, Adv. Appl. Microbiol. 37 (1992) 1–9.
[11] J.C. Spain, Biodegradation of nitroaromatic compounds, Annu. Rev. Microbiol. 49 (1995) 523–555.
[12] B. Bhushan, A. Chauhan, S.K. Samanta, R.K. Jain, Kinetics of biodegradation of *p*-nitrophenol by different bacteria, Biochem. Biophys. Res. Commun. 274 (2000) 626–630.
[13] K. Westerberg, A.M. Elvang, E. Stackebrandt, J.K. Jansson, *Arthrobacter chlorophenolicus* sp. nov., a new species capable of degrading high concentrations of 4-chlorophenol, Int. J. Syst. Evol. Microbiol. 50 (2000) 2083–2092.
[14] M. Martin-Hernandez, J. Carrera, J. Perez, M.E. Suarez-Ojeda, Enrichment of a K-strategist microbial population able to biodegrade *p*-nitrophenol in a sequencing batch reactor, Water Res. 43 (2009) 3871–3883.
[15] F. Rezouga, M. Hamdi, M. Sperandio, Variability of kinetic parameters due to biomass acclimation: case of *para*-nitrophenol biodegradation by stirred tank bioreactor, Bioresour. Technol. 100 (2009) 5021–5029.
[16] L. Xing-Yu, W. Bao-Jun, J. Cheng-Ying, Z. Ke-Xin, H.L. Drake, L. Shuang-Jiang, Simultaneous biodegradation of nitrogen-containing aromatic compounds in a sequencing batch bioreactor, J. Environ. Sci. 19 (2007) 530–535.
[17] M.C. Tomei, M.C. Annesini, S. Bussoletti, 4-Nitrophenol biodegradation in a sequencing batch reactor: kinetic study and effect of filling time, Water Res. 38 (2004) 375–384.
[18] S.H. Israni, S.S. Koli, A.W. Patwardhan, J.S. Melo, S.F. Dsouza, Phenol degradation in rotating biological contactors, J. Chem. Technol. Biotechnol. 77 (2002) 1050–1057.
[19] S.Y. Lee, Y. Pang-Tsui, Succeed at gas/liquid contacting, Chem. Eng. Prog. 95 (1999) 23–49.
[20] J.U. Kreft, J.W.T. Wimpenny, Effect of EPS on biofilm structure and function as revealed by an individual-based model of biofilm growth, Water Sci. Technol. 43 (2001) 135–141.
[21] B.A. Meyer, D.W. Smith, Flow through porous media: comparison of consolidated and unconsolidated materials, Ind. Eng. Chem. Fundam. 24 (1985) 360–368.
[22] G. Radilla, M. Fourar, F. Larachi, Correlating gas-liquid co-current flow hydrodynamics in packed beds using the F-function concept, J. Chem. Technol. Biotechnol. 80 (2005) 107–112.
[23] M.M. Bradford, Rapid and sensitive method for the quantitation of microgram quantities of protein utilizing the principle of protein-dye binding, Anal. Biochem. 72 (1976) 248–254.
[24] APHA, Standard Methods for the Examination of Water and Wastewater, 20th ed., Washington, DC, 1998.
[25] S. Eker, F. Kargi, Performance of a hybrid-loop bioreactor system in biological treatment of 2,4,6-tri-chlorophenol containing synthetic wastewater: effects of hydraulic residence time, J. Hazard. Mater. 144 (2007) 86–92.
[26] D.S. Hodge, J.S. Devinny, Modeling removal of air contaminants by biofiltration, J. Environ. Eng. 121 (1995) 21–32.
[27] A. Gomez-DeJesus, F.J. Romano-Baez, L. Leyva-Amezcua, C. Juarez-Ramırez, N. Ruiz-Ordaz, J. Galındez-Mayer, Biodegradation of 2,4,6-trichlorophenol in a packed-bed biofilm reactor equipped with an internal net draft tube riser for aeration and liquid circulation, J. Hazard. Mater. 161 (2009) 1140–1149.
[28] H. Taguchi, A.E. Humphrey, Dynamic measurement of the volumetric oxygen transfer coefficients in fermentation systems, J. Ferment. Technol. 44 (1996) 881–889.
[29] J.M.T. Vasconcelos, J.M.L. Rodrigues, S.C.P. Orvalho, S.S. Alves, R.L. Mendes, A. Reis, Effect of contaminants on mass transfer coefficients in bubble column and airlift contactors, Chem. Eng. Sci. 58 (2003) 1431–1440.
[30] F. Fava, D. Di Gioia, L. Marehetti, G. Quattroni, Aerobic dechlorination of low-chlorinated biphenyls by bacterial biofilms in packed-bed batch bioreactors, Appl. Microbiol. Biotechnol. 45 (1996) 562–568.
[31] N.K. Sahoo, K. Pakshirajan, P.K. Ghosh, Enhancing the biodegradation of 4-chlorophenol by *Arthrobacter chlorophenolicus A6* via medium development, Int. Biodet. Biodeg. 64 (2010) 474–480.
[32] M. Alexandar, B.K. Lustigman, Effect of chemical structure on microbial degradation of substituted benzenes, J. Agric. Food Chem. 14 (1966) 410–413.
[33] R.K. Costura, P.J.J. Alvarez, Expression and longevity of toluene dioxygenase in *Pseudomonas putida f1* induced at different dissolved oxygen concentrations, Water Res. 34 (2000) 3014–3018.
[34] N.K. Sahoo, K. Pakshirajan, P.K. Ghosh, A. Ghosh, Biodegradation of 4-chlorophenol by *Arthrobacter chlorophenolicus A6*: effect of culture conditions and degradation kinetics, Biodegradation 22 (2011) 275–286.
[35] S.K. Ajmera, C. Delattre, M.A. Schmidt, K.F. Jensen, Micro fabricated cross-flow chemical reactor for catalyst testing, Sens. Actuat. B: Chem. 82 (2002) 297–306.
[36] D. Fassnacht, R. Portner, Experimental and theoretical considerations on oxygen supply for animal cell growth in fixed-bed reactors, J. Biotechnol. 72 (1999) 169–184.
[37] M. Chern, Y. Chien, Competitive adsorption of benzoic acid and *p*-nitrophenol onto activated carbon: isotherm and breakthrough curves, Water Res. 37 (2003) 2347–2356.
[38] P.L. TenBrook, S.M. Kendall, R.S. Tjeerdema, Toxicokinetics and biotransformation of *p*-nitrophenol in white sturgeon (*Acipenser transmontanus*), Ecotoxicol. Environ. Saf. 64 (2006) 362–368.
[39] P. Jiang, J. Zhou, A. Zhang, Y. Zhong, Electrochemical degradation of *p*-nitrophenol with different processes, J. Environ. Sci. 22 (2010) 500–506.
[40] U. Lendenmann, J.C. Spain, B.F. Smets, Simultaneous degradation of 2,4-dinitrotoluene and 2,6-dinitrotoluene in an aerobic fluidized bed biofilm reactor, Environ. Sci. Technol. 32 (1998) 82–87.
[41] M.D. Shelley, R.L. Autenrieth, J.R. Wild, B.E. Dale, Thermodynamics analysis of trinitrotoluene biodegradation and mineralization pathways, Biotechnol. Bioeng. 50 (1996) 198–205.
[42] J.W. Costerton, Z. Lewandowski, D.E. Caldwell, D.R. Korber, H.M. Lappin-Scott, Microbial biofilms, Annu. Rev. Microbiol. 49 (1995) 711–745.
[43] Z. Salehi, H. Yoshikawa, R. Mineta, Y. Kawase, Aerobic biodegradation of *p*-nitrophenol by acclimated waste activated sludge in a slurry bubble column, Proc. Biochem. 46 (2011) 284–289.
[44] Y. Zheng, D. Liu, H. Xu, Y. Zhong, Y. Yuan, L. Xiong, W. Li, Biodegradation of *p*-nitrophenol by *Pseudomonas aeruginosa HS-D38* and analysis of metabolites with HPLC-ESI/MS, Int. Biodet. Biodeg. 63 (2009) 1125–1129.
[45] R.K. Jain, J.H. Dreisbach, J.C. Spain, Biodegradation of *p*-nitrophenol via 1,2,4-benzenetriol by an Arthrobacter, Appl. Environ. Microbiol. 60 (1994) 3030–3032.
[46] J.L. Matthew, A. McMahon, J. Daugulis, Enhancement of biogenic sulfide production in a packed-bed bioreactor via critical inoculum design and carrier material selection, Biotechnol. Bioeng. 100 (2008) 855–863.
[47] K. Karim, S.K. Gupta, Biotransformation of nitrophenols in upflow anaerobic sludge blanket reactors, Bioresour. Technol. 80 (2001) 179–186.
[48] M.C. Tomei, M.C. Annesini, S. Rita, A.J. Daugulis, Biodegradation of 4-nitrophenol in a two-phase sequencing batch reactor: concept demonstration, kinetics and modelling, Appl. Microbiol. Biotechnol. 80 (2008) 1105–1112.
[49] Y.G. Cho, S.K. Rhee, S.T. Lee, Influence of phenol on biodegradation of *p*-nitrophenol by freely suspended and immobilized *Nocardioides* sp. NSP41, Biodegradation 11 (2000) 21–28.